

space group $I2/a$. In this form the molecule has a C_2 axis with CCSS torsion angles of $-167.4 (2)^\circ$ and a CSSC torsion angle of $-86.3 (1)^\circ$. Form II is obtained from a wide variety of organic solvents or when an aqueous solution of the compound is evaporated quickly. Mixtures of forms I and II are obtained when aqueous solutions are evaporated on the time scale of days.

Form II crystallizes in the space group $P\bar{1}$, with no molecular symmetry elements. The CCSS torsion angles are $-76.2 (5)^\circ$ and $-64.4 (6)^\circ$, and the CSSC torsion angle is $-92.3 (4)^\circ$. Apart from the carboxyl groups, the bond distances and bond angles in the two forms are quite similar. Versus the corresponding dimensions in form I, one CS bond in form II is longer by 0.02 \AA and the SSC angle involving that carbon is larger by 3.1° . The SCC angle on the other end of form II exceeds that in form I by 4° .

The carboxyl groups in form I are unexceptional, with their planes essentially coincident with the SCC planes. The carboxyl group on the end of form II having the longer CS bond has reasonably normal dimensions, but it is twisted, with an SCCO torsion angle of $-79.1 (9)^\circ$ to the carbonyl oxygen atom. The other end of form II displays a statistical disordering of the oxygen atoms that is best interpreted as two alternative orientations for the carboxyl group: one that is coplanar with SCC and one that is rotated away from coplanarity by $64 (2)^\circ$. Such a disordering avoids several short O-O contacts that would otherwise occur if the molecules were to adopt one or the other orientation exclusively. Because of the disorder, however, the bond distances and angles in this group are less reliable.

The Raman spectra of authentic samples of crystalline forms I and II show significant differences, particularly in the $200\text{--}800\text{-cm}^{-1}$ region. For form I we find such spectral lines (with subjective intensities) at $194 (s)$, $250 (m)$, $292 (w)$, $402 (vs)$, $422 (m)$, $536 (vs)$, $563 (w)$, $651 (w)$, and $799 (vs) \text{ cm}^{-1}$. The corresponding portion of the spectrum of form II has lines at $182 (sh)$, $235 (w)$, $269 (m)$, $290 (w)$, $422 (w)$, $434 (w)$, $510 (vs)$, $550 (w)$, $570 (w)$, $582 (m)$, $664 (s)$, $766 (w)$, and $786 (w) \text{ cm}^{-1}$.

In their original article Van Wart and Scheraga⁶ report Raman lines for their sample of dithiodiglycolic acid as follows: $270 (m)$, $293 (w)$, $419 (w)$, $431 (w)$, $481 (w)$, $508 (vs)$, $549 (w)$, $569 (w)$, $581 (m) \text{ cm}^{-1}$. A comparison of these results with ours leaves little doubt that the unspecified recrystallization procedure to which they subjected their commercial sample of this compound gave a form II product. Since their interpretation of the conformational dependence of the disulfide stretching frequency was predicated on the assumption that they had studied form I, we must now conclude that the Van Wart and Scheraga model is no longer credible. The actual disulfide stretching frequency in form I does, however, closely approximate the 540-cm^{-1} value predicted by the Sugeta, Go, and Miyazawa correlation scheme.

Normal coordinate calculations were then used to establish that the spectral differences between forms I and II indeed have a conformational origin. With the realization that the results cannot be strictly correct, owing to the fact that in both crystals the carboxyl groups form hydrogen-bonded dimers, the spectrum of crystalline form I was fitted with a Fletcher-Powell¹¹ optimized Urey-Bradley force field. The starting force constants were taken from Sugeta⁵ for the CH_2SSCH_2 portion of the molecule and from Nakamoto and Kishida¹² for the in-plane motions of the carboxyl group. The out-of-plane bending force constant was estimated from the results of Brooks and Haas.¹³ No force constant changed by more than 15% upon optimization of the force field.

When the optimized force field was used to calculate the spectrum of an isolated molecule having the form I geometry, the calculated disulfide stretching frequency was 532 cm^{-1} . The same force field then gave a calculated disulfide stretching frequency of 510 cm^{-1} for an isolated molecule having the geometry of either of the form II rotamers. These results strongly support the validity of the Sugeta, Go, and Miyazawa model of the conformational dependence of the disulfide stretching frequency.

Acknowledgment. The work done at the Roswell Park Memorial Institute was supported by the National Institutes of Health (CA23704).

Supplementary Material Available: Tables I-VI giving crystal data and data collection parameters, positional and thermal parameters, and selected bond distances, bond angles, and torsion angles for forms I and II of dithiodiglycolic acid (6 pages). Ordering information is given on any current masthead page.

Synthesis and Characterization of Dirhodium Complexes with Four N,N' -Diphenylbenzamidine Bridging Ligands. Electrochemical Generation and ESR Properties of $[\text{Rh}_2(\text{N}_2\text{R}_2\text{CR})_4]^n$ Where R = Phenyl and $n = 1$ and -1

J. C. Le, M. Y. Chavan, L. K. Chau, J. L. Bear,* and K. M. Kadish*

Department of Chemistry
University of Houston—University Park
Houston, Texas 77004

Received August 21, 1985

The syntheses and characterizations of a large number of dirhodium(II) complexes have been reported. Studies include the well-characterized dirhodium carboxylates, $\text{Rh}_2(\text{O}_2\text{CR})_4$,^{1,2} as well as dirhodium complexes with mixed bridging ligands such as $\text{Rh}_2(\text{O}_2\text{CR})_n(\text{R}'\text{NOCR})_{4-n}$ ³⁻⁷ and $[\text{LRh}_2(\text{O}_2\text{CR})_3]^+$ where L is a neutral bridging ligand which binds through two nitrogen donors.⁸

Dirhodium complexes with carboxylate bridging ligands undergo only a single oxidation, but complexes containing the more basic amidate bridging ions may undergo two reversible oxidations corresponding to the formation of a formal Rh(II,III) and Rh-(III,III) species.³⁻⁷ The reversible formation of a formal Rh(II,I) species has not been observed for the reduction of any neutral dirhodium(II) complexes. This oxidation state appears to be accessible⁸ during electrochemical reduction of the positively charged $[\text{LRh}_2(\text{O}_2\text{CCH}_3)_3]^+$ and may also be observed as a transient intermediate during the irreversible reduction of $\text{Rh}_2(\text{O}_2\text{CR})_4$.⁹ However, no spectral characterization of dirhodium(II,I) complexes has been reported.

Numerous theoretical studies on dirhodium(II) complexes have been published (see ref 1, 2) but no experimental data exist on the LUMO of these complexes. Thus, the synthesis of a neutral dirhodium(II) complex which may be reversibly reduced to $\text{Rh}_2(\text{II,I})$ is of some interest. We have now synthesized such a complex using N,N' -diphenylbenzamidine. This dirhodium(II) complex is represented by the formula $\text{Rh}_2(\text{N}_2\text{R}_2\text{CR})_4$ where R = phenyl. This is the first reported dirhodium(II) complex with this class of bridging groups. The complex is oxidized and reduced by reversible one-electron transfer processes and a characterization of the products is possible by ESR spectroscopy.

Tetrakis(benzamidinato)dirhodium(II) was the major product obtained from the reaction of $\text{Rh}_2(\text{O}_2\text{CCH}_3)_4$ with benzamidine. The general procedure has previously been described in the literature for substitution reactions involving amide ligands.⁷ The

(1) Boyer, E. B.; Robinson, S. D. *Coord. Chem. Rev.* **1983**, *50*, 109.

(2) Felthouse, T. R. *Prog. Inorg. Chem.* **1982**, *29*, 73.

(3) Duncan, J.; Malinski, T.; Zhu, T. P.; Hu, Z. S.; Kadish, K. M.; Bear, J. L. *J. Am. Chem. Soc.* **1982**, *104*, 5507.

(4) Bear, J. L.; Zhu, T. P.; Malinski, T.; Dennis, A. M.; Kadish, K. M. *Inorg. Chem.* **1984**, *23*, 674.

(5) Kadish, K. M.; Lancon, D.; Bear, J. L. *Inorg. Chem.* **1982**, *21*, 2987.

(6) Chavan, M. Y.; Zhu, T. P.; Lin, X. Q.; Ahsan, M. Q.; Bear, J. L.; Kadish, K. M. *Inorg. Chem.* **1984**, *23*, 4538.

(7) Zhu, T. P.; Ahsan, M. Q.; Malinski, T.; Kadish, K. M.; Bear, J. L. *Inorg. Chem.* **1984**, *23*, 2.

(8) Tikkanen, W. R.; Binamira-Soriago, E.; Kaska, W. C.; Ford, P. C. *Inorg. Chem.* **1983**, *22*, 1148.

(9) Das, K.; Kadish, K. M.; Bear, J. L. *Inorg. Chem.* **1978**, *17*, 930 and references therein.

(11) Fletcher, R.; Powell, M. J. D. *Comput. J.* **1963**, *6*, 163-168.

(12) Nakamoto, K.; Kishida, S. *J. Chem. Phys.* **1964**, *41*, 1554-1558.

(13) Brooks, W. V. F.; Haas, C. M. *J. Phys. Chem.* **1967**, *71*, 650-655.

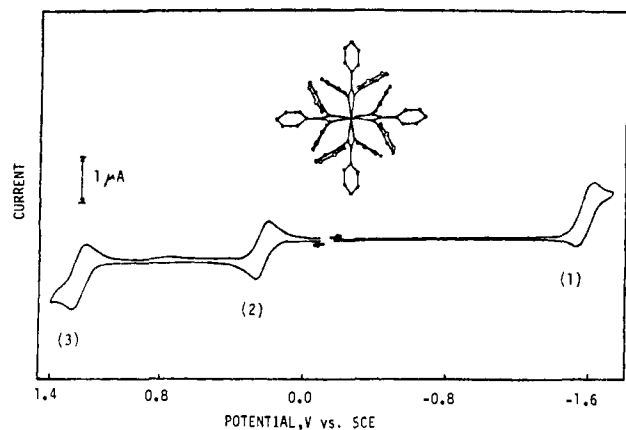
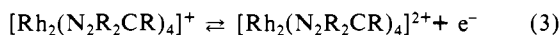
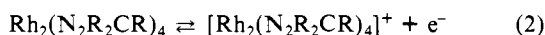
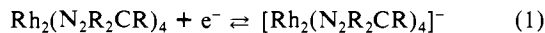


Figure 1. Crystal structure viewed along the Rh-Rh axis and cyclic voltammogram of $\text{Rh}_2(\text{N}_2\text{R}_2\text{CR})_4$ in CH_2Cl_2 , 0.1 M TBAP. Scan rate = 50 mV/s.

crystal and molecular structure (shown in Figure 1) was also determined. The Rh-Rh and Rh-N distances are 2.389 and 2.050 Å, respectively. The complex crystallizes in the space group $P_{4/n}$ with D_4 molecular symmetry and has a N-Rh-Rh-N torsional angle of 17.3° . There are no axial ligands present in the crystalline state. The visible spectrum of $\text{Rh}_2(\text{N}_2\text{R}_2\text{CR})_4$ in CH_2Cl_2 shows three bands at 845 ($\epsilon \times 10^3$), 590 ($\epsilon \times 10^2$), and 515 nm ($\epsilon \times 10^3$).

Figure 1 shows the cyclic voltammograms of $\text{Rh}_2(\text{N}_2\text{R}_2\text{CR})_4$ in CH_2Cl_2 . A similar voltammogram is obtained in CH_3CN . In both solvents three redox processes are observed. These occur at -1.58, 0.23, and 1.24 V vs. SCE in CH_2Cl_2 and at -1.52, 0.05, and 1.08 V vs. SCE in CH_3CN . Each of the processes corresponds to the addition or abstraction of a single electron so that the overall electrochemistry in CH_2Cl_2 may be represented by the following equations:



A similar sequence of reactions also occurs in CH_3CN but, in this solvent, one or more CH_3CN molecules may be bound to the various complexes. Both reactions 2 and 3 are reversible in the two solvents as evidenced by an $E_{pa} - E_{pc} = 60 \pm 5$ mV. However, the reduction (reaction 1) may be classified as electrochemically quasi-reversible since values of $E_{pa} - E_{pc}$ were equal to 90 ± 5 mV. Whereas two oxidations are predictable from previous studies,⁶⁻⁷ the appearance of a reversible reduction is totally unexpected. The potentials for the first and second oxidation of $\text{Rh}_2(\text{N}_2\text{R}_2\text{CR})_4$ are negatively shifted by 290 and 460 mV in acetonitrile from those observed for $\text{Rh}_2(\text{NROCCH}_3)_4$ where R = phenyl.⁴ Based on these negative shifts one might not expect to observe the presence of a reversible reduction for $\text{Rh}_2(\text{N}_2\text{R}_2\text{CR})_4$ since this process is not observed for $\text{Rh}_2(\text{NROCCH}_3)_4$.

Controlled-potential electrolysis was carried out, and the products of reactions 1 and 2 were monitored by ESR spectroscopy. Figure 2 illustrates the ESR spectra of $[\text{Rh}_2(\text{N}_2\text{R}_2\text{CR})_4]^+$ in CH_2Cl_2 and CH_3CN in frozen glass. These spectra are qualitatively similar to those observed for $[\text{Rh}_2(\text{O}_2\text{CCH}_3)_n(\text{RNOCR})_{4-n}]^+$ in CH_3CN or acetone^{4,6} (although the g values differ substantially). In CH_2Cl_2 (Figure 2a) the complex has a $g_{\perp} = 2.060$ and a $g_{\parallel} = 1.978$. The g_{\parallel} is split into a 1:2:1 triplet by two equivalent rhodium nuclei ($A_{\parallel} = 19.5 \times 10^{-4} \text{ cm}^{-1}$). Similar triplets for other dirhodium(II,III) complexes have been reported in the literature.^{4,6,10} The ESR spectrum of $[\text{Rh}_2(\text{N}_2\text{R}_2\text{CR})_4]^+$ in CH_3CN is unique in that it shows nonequivalent rhodium centers. For example, in CH_3CN (Figure 2b), $[\text{Rh}_2-$

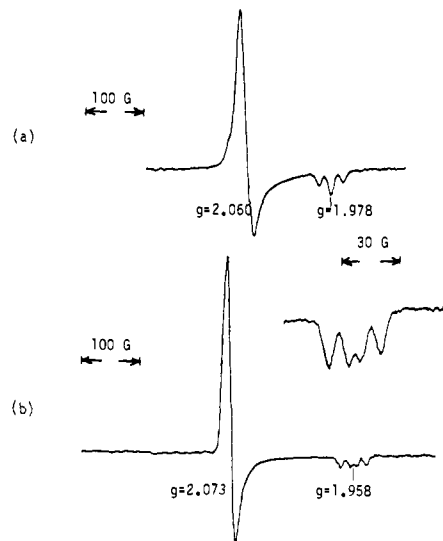


Figure 2. ESR spectra of $[\text{Rh}_2(\text{N}_2\text{R}_2\text{CR})_4]^+$ at -150°C in (a) CH_2Cl_2 , 0.1 M TBAP, and (b) CH_3CN , 0.1 M TBAP.

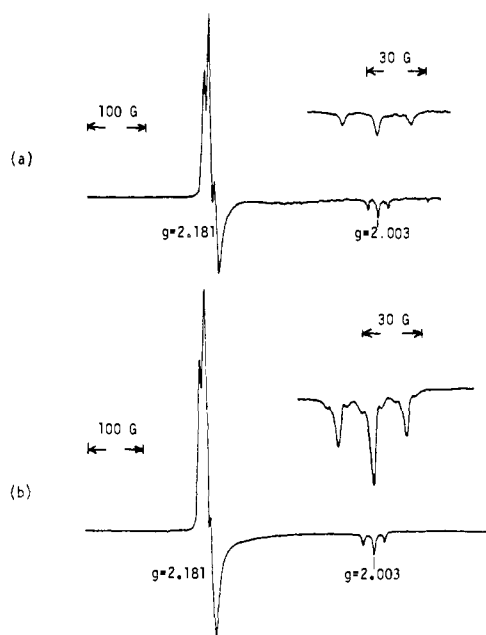


Figure 3. ESR spectra of $[\text{Rh}_2(\text{N}_2\text{R}_2\text{CR})_4]^-$ at -150°C in (a) CH_2Cl_2 , 0.1 M TBAP, and (b) CH_3CN , 0.1 M TBAP.

$(\text{N}_2\text{R}_2\text{CR})_4]^+$ has a $g_{\perp} = 2.073$ and a $g_{\parallel} = 1.958$. The g_{\parallel} is split into a doublet of doublets ($A_{\parallel} = 24.0 \times 10^{-4}$ and $16.0 \times 10^{-4} \text{ cm}^{-1}$) presumably due to the presence of two nonequivalent rhodium nuclei. This nonequivalency might occur if only one of the two Rh atoms of $[\text{Rh}_2(\text{N}_2\text{R}_2\text{CR})_4]^+$ were bound to a CH_3CN molecule. Indeed, electrochemical monitoring of CH_3CN addition to the oxidized species provides evidence that only monoligated complexes are formed at room temperature.¹¹ However, it is important to note that the g_{\parallel} signals show no superhyperfine interaction with the nitrogen of axially bound acetonitrile.

The ESR signal for electrochemically generated $[\text{Rh}_2(\text{N}_2\text{R}_2\text{CR})_4]^-$ is shown in Figure 3.¹² Almost identical spectra are obtained in CH_2Cl_2 and CH_3CN and in both solvents the

(10) Kawamura, T.; Fukamachi, K.; Haysashida, S.; Yonezawa, T. *J. Am. Chem. Soc.* **1981**, *103*, 364.

(11) The formation constant for $[\text{Rh}_2(\text{N}_2\text{R}_2\text{CR})(\text{CH}_3\text{CN})]^+$ is small, and in CH_2Cl_2 containing CH_3CN , a value of $K_f \approx 3 \times 10^1$ is obtained. A second CH_3CN addition does not occur at room temperature in CH_2Cl_2 but the possibility of bis ligand adducts cannot be ruled out in pure CH_3CN at low temperatures.

(12) The singly reduced species is quite stable under the application of a constant potential of -1.7 V, but when the potential is turned off, or the sample is exposed to trace amounts of O_2 , a rapid oxidation and/or decomposition of $[\text{Rh}_2(\text{N}_2\text{R}_2\text{CR})_4]^-$ occurs.

reduced complex has a $g_{\perp} = 2.181$ and a $g_{\parallel} = 2.003$. Both signals are split into triplets ($A_{\perp} = 9 \times 10^{-4} \text{ cm}^{-1}$ and $A_{\parallel} = 16 \times 10^{-4} \text{ cm}^{-1}$). In CH_3CN superhyperfine lines (triplets) are observed in the g_{\parallel} of $[\text{Rh}_2(\text{N}_2\text{R}_2\text{CR})_4]^-$ (Figure 3b) and may be due to a coupling of one ^{14}N nucleus ($I = 1$) of CH_3CN . However, the fact that identical g values (± 0.002) and splittings are obtained in a bonding and a nonbonding solvent suggests that there may be no interaction between the negatively charged dirhodium(II,I) complex and the solvent.

The $g_{\parallel} = 2.003$ for $[\text{Rh}_2(\text{N}_2\text{R}_2\text{CR})_4]^-$ is consistent with the prediction that an unpaired electron in a $\sigma_{\text{M-M}}$ -type orbital should have $g_{\parallel} \approx g_e$.¹⁰ The LUMO of $\text{Rh}_2(\text{O}_2\text{CR})_4$ complexes with weak or no axial ligands has generally been believed to be a σ^* Rh-Rh orbital with little or no contribution from the σ^* Rh-axial ligand.^{10,13-16} Thus, in spite of the differences between $\text{Rh}_2(\text{O}_2\text{CR})_4$ and $\text{Rh}_2(\text{N}_2\text{R}_2\text{CR})_4$, the LUMO of $\text{Rh}_2(\text{N}_2\text{R}_2\text{CR})_4$ appears to be primarily σ^* Rh-Rh. If this is the case, the superhyperfine structure in the g_{\parallel} of Figure 3b may be due to a minor contribution from σ^* Rh-L where L = CH_3CN .

Acknowledgment. The support of the Robert A. Welch Foundation (K.M.K. Grant E-680, J.L.B. Grant E-918) is gratefully acknowledged.

(13) Bursten, B. E.; Cotton, F. A. *Inorg. Chem.* **1981**, 3042 and references therein.

(14) Norman, J. G., Jr.; Kolari, H. J. *J. Am. Chem. Soc.* **1978**, 100, 791.

(15) Norman, J. G., Jr.; Renzoni, G. E.; Case, D. A. *J. Am. Chem. Soc.* **1979**, 101, 5256.

(16) Drago, R. S.; Tanner, S. P.; Richmann, R. M.; Long, J. R. *J. Am. Chem. Soc.* **1979**, 1001, 2897.

Simplification of ^1H NMR Spectra by Selective Excitation of Experimental Subspectra

Donald G. Davis and Ad Bax*

Laboratory of Chemical Physics
Institute of Arthritis, Diabetes, and
Digestive and Kidney Diseases
National Institutes of Health
Bethesda, Maryland 20205

Received July 8, 1985

We propose a new method for the simplification of ^1H NMR spectra by the generation of experimental subspectra. The method is based on the concept of spin propagation¹⁻⁶ via a homonuclear Hartmann-Hahn coherence transfer process^{6,7} and is the improved one-dimensional (1D) analogue of the 2D HOHAHA experiment, described previously.³ For spectra of limited complexity, 1D versions of 2D experiments can have significant advantages over the 2D experiment because of shorter minimum measuring time, reduced data storage requirements, and improved digital resolution.

The basic idea is to invert the resonances of an isolated spin multiplet with a selective 180° pulse and then to let this inverted magnetization propagate through the ^1H coupling network. A difference spectrum (with the decoupler switched off during the selective pulse interval) then yields a subspectrum of all hydrogens

(1) Weitekamp, D. P.; Garbow, J. R.; Pines, A. *J. Chem. Phys.* **1982**, 77, 2870.

(2) Braunschweiler, L.; Ernst, R. R. *J. Magn. Reson.* **1983**, 53, 521.

(3) Davis, D. G.; Bax, A. *J. Am. Chem. Soc.* **1985**, 107, 2820.

(4) Caravatti, P.; Braunschweiler, L.; Ernst, R. R. *Chem. Phys. Lett.* **1983**, 100, 305.

(5) Chandrakumar, N.; Subramanian, S. *J. Magn. Reson.* **1985**, 62, 346.

(6) Bax, A.; Davis, D. G. In "Advanced Magnetic Resonance Techniques in Systems of High Molecular Complexity"; Nicolai, N., Valensin, G., Eds.; Birkhauser: Basel, in press.

(7) Bax, A.; Davis, D. G. *J. Magn. Reson.* **1985**, 63, 207.

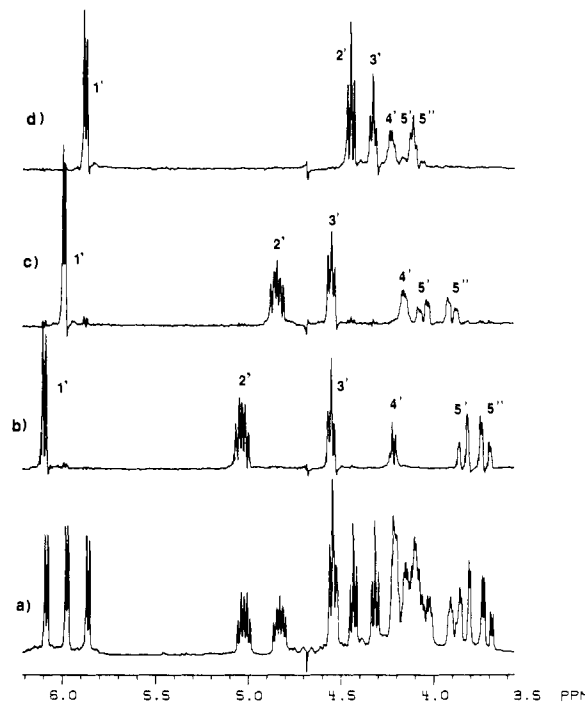


Figure 1. Spectra, 270 MHz, of the ribose region of $\text{A}2'\text{-P-}5'\text{A}2'\text{-P-}5'\text{A}$. (a) Regular spectrum; (b-d) selective excitation subspectra of $\text{A}2'\text{-P}$, $\text{P-}5'\text{A}2'\text{-P}$, and $\text{P-}5'\text{A}$ nucleotides. For all three difference spectra, propagation was started at the anomeric proton and a propagation delay of 180 ms was used.

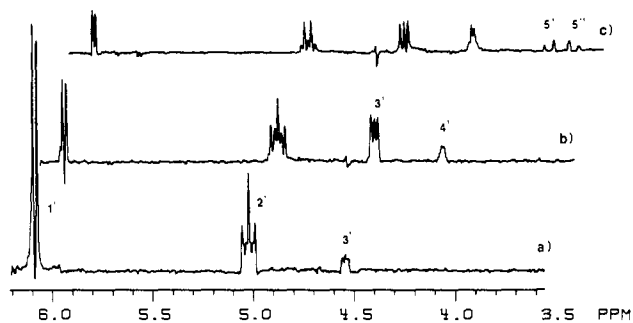


Figure 2. Propagation subspectra of the ribose ring of the $\text{A}2'\text{-P}$ nucleotide, obtained for propagation times of (a) 40, (b) 80, and (c) 120 ms. Spectra b and c are horizontally displaced to improve the visual appearance. For increasing propagation delay, the $1'$ proton magnetization propagates into the $5',5''$ direction at a rate determined by the various coupling constants between vicinal protons.

directly or indirectly scalar coupled to the inverted ^1H resonance. By studying the subspectrum as a function of propagation time, a straightforward spectral assignment within the subunit is obtained.

We demonstrate the method for the trinucleotide $\text{A}2'\text{-P-}5'\text{A}2'\text{-P-}5'\text{A}$, a potent inhibitor of protein synthesis. The regular 270-MHz ^1H spectrum (Figure 1a) of the ribose region shows a substantial amount of overlap. The anomeric protons, however, are well separated in the 5.85-6.1 ppm region and serve as labels that can separately be inverted by a frequency-selective 180° pulse. By use of 180-ms propagation periods, the experimental subspectra of the three ribose rings (Figure 1b-d) were obtained by starting the propagation from the anomeric protons. The individual rings are also readily identified: $\text{H}2'$ in Figure 1d is a triplet and does not show coupling to ^3P , assigning this spectrum to the $\text{P-}5'\text{A}$ nucleotide. Similarly, the $\text{H}5'$ and $\text{H}5''$ resonances in Figure 1b (when examined at higher resolution than shown) do not exhibit coupling to ^3P , assigning this spectrum to $\text{A}2'\text{-P}$.

Spectral assignment within each subspectrum can be obtained by variation of the duration of the propagation period. For short propagation times (~ 40 ms) magnetization has not propagated